Combustion Modeling in Solid Rocket Motor Plumes

Tobias Ecker⋆†*, Sebastian Karl*⋆ *and Klaus Hannemann*⋆
⋆ *German Aerospace Center (DLR)*
Institute of Aerodynamics and Flow Technology
Bunsenstr. 10, Göttingen, Germany
tobias.ecker@dlr.de · sebastian.karl@dlr.de · klaus.hannemann@dlr.de
†Corresponding author

Abstract

The thermo-chemistry of plumes emanating from solid rocket motors (SRM) is strongly influenced by hydrogen/oxygen/chlorine chemistry. These after-burning reactions have a significant impact onto the infrared signature, as well as on chemical and thermal loads within the propulsion system. This study provides an overview on available combustion mechanism and evaluate their applicability to CFD. Based on the results an improved skeletal kinetic model is proposed and validated against detailed mechanisms. The results of this study offer an evaluation of the performance of current finite rate chemistry models and the impact on flowfield characteristics of SRM plumes.

1. Introduction

Plumes emanating from solid rocket motors (SRM) exhibit flow statistics strongly influenced by complex hydrogen/oxygen/chlorine chemistry. These after burning reactions within the plume have a significant impact onto the infrared (IR) irradiance signature, as well as on the chemical erosion of any active or passive mechanical steering system exposed to the reactive motor plume. As SRM combustion chambers operate at oxidizer-fuel ratios considerably less than stoichiometric, afterburning within the plume shear layer occurs. Asides from the intermediate thermochemical loads of the plume on the launch vehicle, the resulting plume exhaust gases of Ammonium perchlorate (AP) based SRM may also have an impact on ozone layer depletion[1,2] in the atmosphere and the biosphere of the launch site.[3] Within this study we provide an overview on the currently available combustion mechanism and evaluate their applicability to SRM plume modeling. For a preliminary evaluation, the performance of the considered mechanisms is evaluated using a constant volume reactor. Based on the results an improved 28 reaction skeletal kinetic model is proposed and validated against detailed mechanisms in constant volume reactor test cases and a counter-flowing diffusion flame. Subsequently, selected mechanisms are applied in Reynolds-averaged Navier-Stokes CFD calculations of a small scale AP/HTPB SRM plume test case. From the evaluation of the plume thermochemistry it can be shown that the proposed model offers improved performance at lower computational costs. The results of this study offer a relevant evaluation of the performance of current SRM finite rate chemistry models and their impact on flowfield characteristics and are helpful for future scale-resolved simulations of multispecies, reactive solid-rocket motor plumes.

2. Combustion kinetics modeling for solid rocket motor plumes

Modeling combustion is a challenging process, modeling solid rocket combustion even more so due to the wide range of physical phenomena involved. Challenges include the chemical complexity of the various single and double base propellants, the influence of the heterogen composition of the fuel grain, as well as wall heatflux on the pyrolysis of the fuel on the grain surface.[4] SRM boosters for large launch vehicles like the Space Shuttle Solid Rocket Boosters (SRBs), Ariane 5 solid boosters (P241/P238), but also launchers with complete SRM based stages like the Vega C, some sounding rockets and tactical missiles (e.g. M51) are often based on mixtures of AP/HTPB/aluminum compositions. Therefore several kinetic models which include chlorine pathways have been proposed for modeling the thermochemical properties of SRM plumes.[2,5,6] Numerical studies of SRM plume flows using computational fluid dynamics (CFD)[2,5–9] and Direct Simulation Monte Carlo (DSMC)[10] - for plumes in hight altitudes - have been conducted in the past with a focus on base plate heat flux, plume thermochemistry and infrared (IR) signatures. Many of these CFD studies have combined reduced finite rate chemistry models of the SRM afterburning with a model for the particle-gas interactions,[2,5,8] which can have an additional heterogeneous effects on the processes in the plume.

COMBUSTION MODELING IN SOLID ROCKET MOTOR PLUMES

Modeling the reaction kinetics in solid rocket motor plumes is a difficult task due to the vast number of species and reaction pathways involved. A kinetic model for this application would include subsets of hydrogen/oxygen/chlorine/carbon oxides and possible nitrogen/nitrogen oxide reactions. There are several finite rate chemistry mechanisms[2,5,6,11,12] which may be suitable for the modeling or haven been used in the past for the modeling of SRM plumes. An overview of the kinetic models in the order of their complexity is given in table 1.

Table 1: Available reaction mechanisms

Mechanism name	No. of reactions	Reference
Troyes (2006)	17	[5]
current[a]	28	
Niu (2017)	30	[9]
Poubeau (2016)	37	[6]
Denison (1994)	46	[2]
Roessler (1992)	56	[11]
Pelucchi (2015)	102	[12]

[a]will be discussed further in section 3

Of these six previously published kinetic models, the models by Denison et al.,[2] Troyes et al.,[5] Poubeau et al.[6] and Niu et al.[9] have been used in past works for modeling the thermo-chemistry of SRM plume flow fields. To the author's knowledge there are currently no published studies in the open literature available which can validate these models against each other or more importantly against experimental results of SRM plumes.

Denison et al.[2] presented a study on the interaction of chlorine based SRM exhaust with the atmosphere and the associated ozone depletion. In their study the authors present several reduced kinetic models for the SRM afterburning chemistry and dispersion in the hot plume and the chemistry and the successive diffusion in the cool plume. The presented hot plume mechanism is based on 46 reactions. For a hypothetical solid rocket motor based on AP, binder and aluminum loading the authors calculated the resulting hot plume with finite rate chemistry and then evaluated the ozone depletion. Their results indicated local ozone depletion to be only present over a very short periods of time.

Troyes et al.[5] presented a skeletal mechanism choosen as a computational efficient compromise based on available models. In their study the authors focus on the numerical simulation of the reactive two-phase flow from the end of the motor combustion chamber to the exhaust plume using both finite rate plume chemistry, as well as models for the aluminium oxide content. In their study Troyes et al. demonstrate the application in a RANS calculation of a SRM plume flow and show the significant afterburning effect due to the chemical reactions between exhaust and air in the jet's shear layer. This kinetic model has been used for several studies[8] on SRM plumes by ONERA since. Poubeau et al.[6] recently published a computational study on performing large eddy simulation (LES) of a SRM plume in conjunction with an offline chemistry model in order to evaluate the impact of SRM plumes on ozone in the earth's atmosphere. The kinetic model used for the offline chemistry is based on a reduced GRI 3.0[13] with additional chlorine pathways. The chemistry is solved based on a constant pressure reactor modelled in CANTERA along streamlines of a time-averaged flowfield of a single inert species in order to determine temperature and chemical species distribution. It should be noted due the nature of the frozen chemistry it is likely that effects of species composition and associated temperature change on the plume flow field itself are not fully captured with this approach. Another kinetic model consisting of 30 reactions has been presented by Niu et al..[9] The model is based on a hdyrogen/oxygen combustion mechanism by Jensen and Jones[14] and extended with pathways for nitrogen and chlorine reactions. In contrast to all other mechanisms presented here nitrogen reaction pathways are considered by the Denison et al.[2] and Niu et al.[9] kinetic model. This is mostly relevant at elevated temperature within the jet core region. The study by Niu et al. details an approach to modeling the afterburning in a SRM plume and successive determination of spectral intensities in the IR bands. The authors found afterburning effects to significantly increase the size and shape of radiance images and good agreement with IR experimental data.

Asides from these kinetic models which have been used for numerical studies on SRM plumes, two other much more detailed models containing the described pathways are available. Roessler et al.[11] presented a study on moist CO oxidation inhibited by trace quantities of HCl. The 56 reactions step mechanism is validated by data from an atmospheric pressure flow reactor. The study is most applicable to SRM plume flows as the combustion chamber products from a typical SRM based on AP/HTPB consist of large quantities of HCl, CO and H_2O.[15] The author's kinetic model seems to be a main inspiration for the skeletal mechanisms previously described. A more detailed model consisting of 102 reactions was recently presented by Pelucchi et al..[12] The authors give a very detailed account on how they have updated on the high temperature chlorine chemistry for an improved $H_2/Cl_2/HCl/CO/O_2$ kinetic model. The presented model is validated against selected experimental data and is the currently most detailed mechanism to describe the

chemistry of chlorine species/fuel interactions – a process directly applicable to SRM plume environments.

2.1 Reactor studies

In order to verify and validate the different reaction mechanisms with their vastly differing amounts of kinetic pathways, several numerical studies on a constant volume reactor were conducted. For the processes in a reacting flow, the rate change of species can be modeled using a finite rate chemistry approach. The rate at which each species changes during a chemical process is determined from the chemical reactions as:[16]

$$\omega_s = M_s \sum_r (\beta_s^r - \alpha_s^r) \left[k_r^f \prod_s (n_s)^{\alpha_s^r} - k_r^b \prod_s (n_s)^{\beta_s^r} \right]$$

where α_s^r and β_s^r are the stoichiometric coefficients for the educt and product for reaction r respectively, k_r^f and k_r^b the forward and backward reaction rate for reaction r respectively, n_s is the molar density and M_s is the molar mass of species s. k_r^f and is the forward reaction rate according to the Arrhenius law

$$k = A\, T^n \exp\left(-\frac{E_a}{RT}\right)$$

where A is the pre-exponential factor, n is the temperature exponent and E_a is the activation energy. The rate constants k_b^f for the reverse reactions are evaluated from the equilibrium constants.

The constant pressure reactor problem is solved by using the CANTERA[17] open-source suite of tools. An overview of the 3 different cases, which include a moist CO/HCl case - similar to actual SRM plume conditions, a H_2/Cl_2 case and a classic stoichiometric hydrogen/oxygen combustion case is given in table 2.

Table 2: Overview reactor test cases.

| Case name	type	T_{start} [K]	p [atm]	X_{start}
Roessler [11]	nozzle flow in N_2	1000.0	1.0	CO: 0.0086, O_2: 0.0053, H_2O: 0.0057, HCl: 0.00019
Lifshitz [18]	shock tube	-	1.0	Ar: 0.792, H_2: 0.104, Cl_2: 0.104
Slack [19]	shock tube	-	1.0	*stoichiometric* H_2 and air

2.2 Reactive moist CO/HCl mixture

The time histories of the mole fractions of selected educts and products within the reactor case are shown in figure 1. For the two most detailed mechanisms (see figure 1a), the mechanism by Roessler et al.[11] and the mechanism by Pelucchi et al.,[12] results are in good agreement with the experimental data by Roessler et al..[11] Most notable is the oxidation of CO to CO_2, which is expected to play a role in most SRM plumes due to the high amount of carbon monoxide in the SRM combustion chamber. From the results a strong influence of species thermodynamic database used for the computations is noticable. Three different publicly available databases were tested, the original NASA CEA database based on NASA 9 polynomials (N9), the thermodynamics database available from the GRI 3.0 mechanism (N7 - GRI) and the thermodynamics database used by Pelucchi et al. (N7 - PEL)[12] which generally gives similar results to the NASA 9 CEA database but is presented in NASA 7 polynomials. For this test case, the original numerical data by Roessler et al.[11] is best reproduced by using the GRI 3.0[13] NASA polynomials. For this comparison the temporal axis of each computational dataset is anchored with an offset on the point where 50% of the final CO_2 concentration is reached, therefore ignoring differences in ignition delay times. The results using the simplified kinetic models by Troyes et al.[5] and Denison et al.[2] are displayed in figure 1b. The changing molar fractions exhibit a general behavior similar to the more detailed model. However strong differences arise on the reactor mixture fractions during the reaction process and the reaction time scales. In terms of species composition the strongest differences are visible in the HCl mole fraction development which exhibits a much stronger drop in comparison to the more detailed models. The kinetic mechanism by Poubeau et al.[6] was also tested but displayed 2-3 longer reaction timescales and was therefore not included in the figure. In order to exclude an transcription error, the original GRI 3.0[13] was reduced to only include the pathways reported by Poubeau. This approach allowed exact reproduction of the behaviour of the Poubeau model. Similar issues were present with the kinetic model by Niu et al.,[9] which is also not included for clarity.

The development of the reactor temperature as predicted by all investigated models is shown in figure 2. As is to be expected the models by Roessler et al.[11] and Pelucchi et al.[12] give the closest agreement to the experimental data.

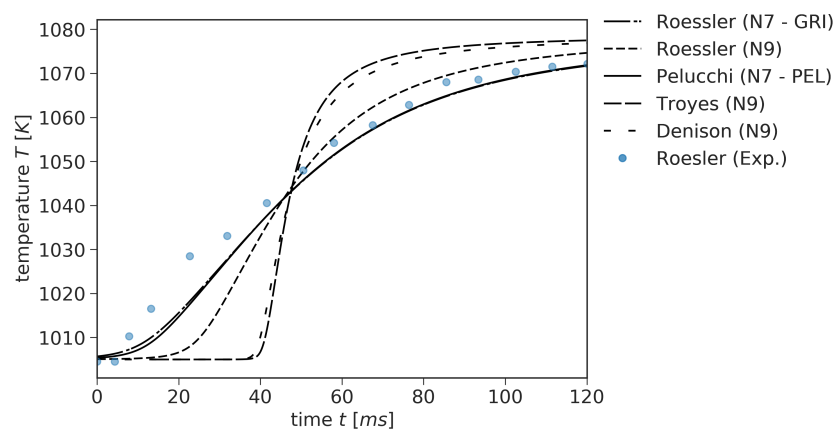COMBUSTION MODELING IN SOLID ROCKET MOTOR PLUMES
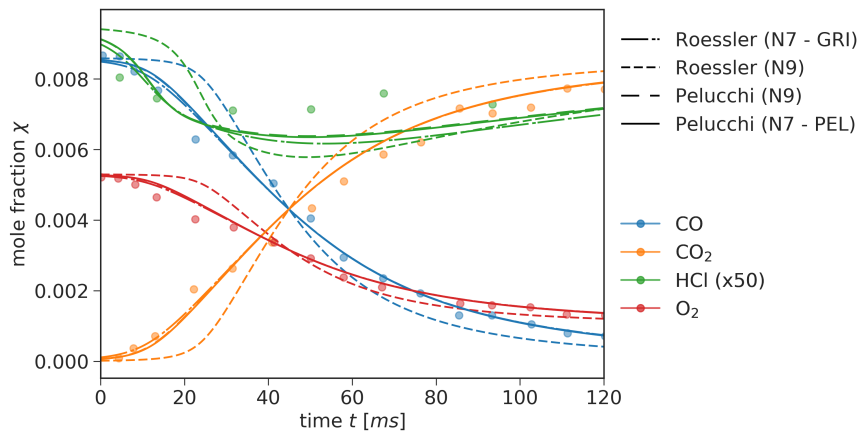
(a) Roessler and Pelucchi reaction kinetics.
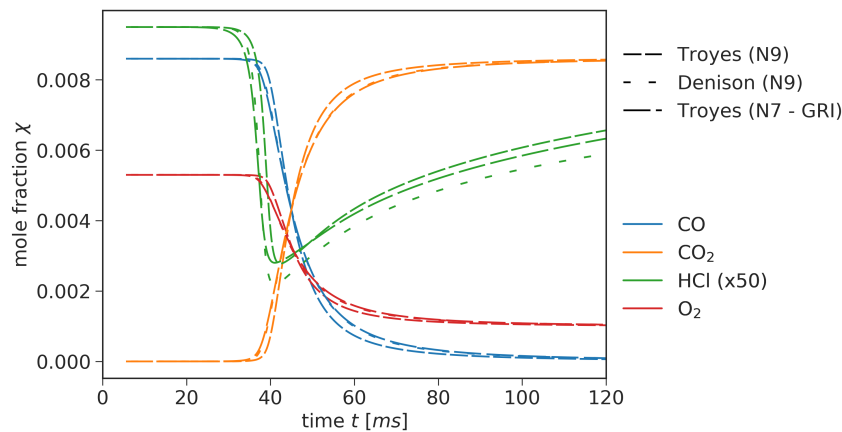
(b) Troyes and Dension reaction kinetics.

Figure 1: Mole fractions of educts and products in Roessler reactor case.

Figure 2: Reactor temperature for moist CO/HCl combustion (Roessler reactor case). Circles indicate the experimental data by Roessler et al.[11]

In an effort to classify the observed deviations in ignition delay times between the mechanism the same reactor conditions were studied at a temperature range representative for non aluminized solid rocket motor exhaust temperatures (1000 - 1800 K). The results of this study are summarized in figure 3. The ignition delay time for this case was defined as the occurence of the maximum amount of hydroxide. As previously noted, the results from the Poubeau et al.[6] kinetic model were excluded from display due to larger differences in reaction time scale. It can be seen that the

strongest deviations between mechanisms are present on the low side of the temperature range and lie in the range of orders of magnitude. On the high range of temperatures (T > 1500 K) the ignition delay times predicted by the different kinetic mechanism cluster in two regions which are different by approximately factor of two. This indicates that the choice of kinetic model may play a larger role in the oxygenated shear layers of the plume and may be less important in the hot potential core region where there is little oxygen present in any case.
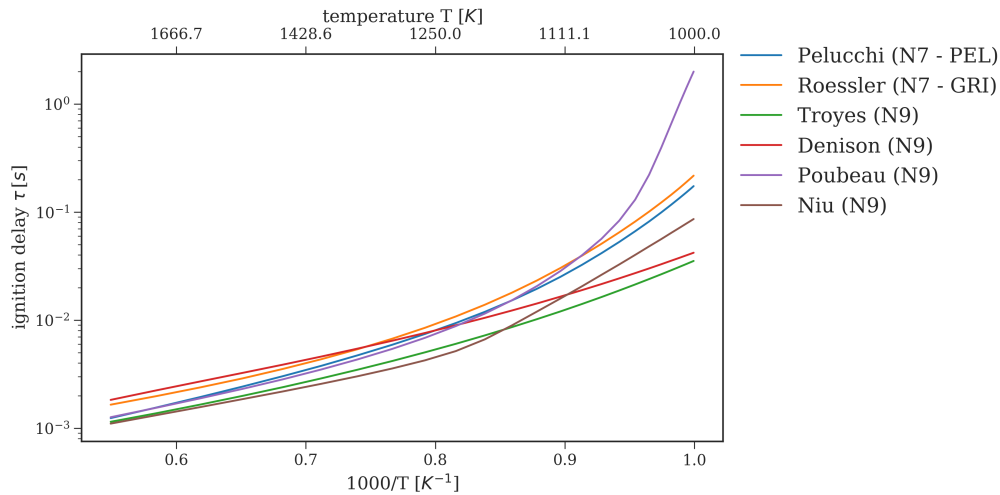
Figure 3: Ignition delay times for moist CO/HCl combustion (Roessler reactor case).
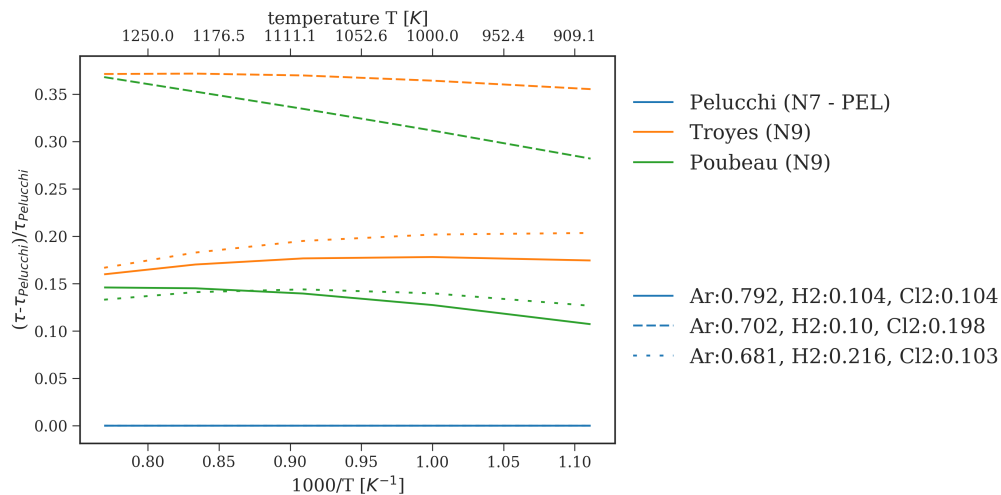
2.3 Reactive H_2/Cl_2 mixture
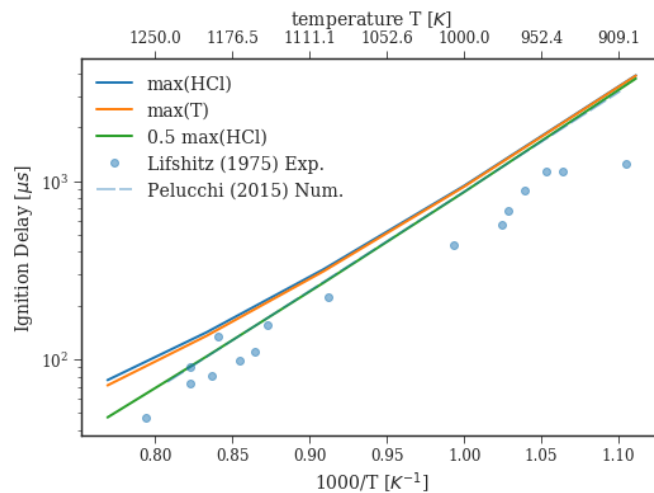
Figure 4: H_2/Cl_2 combustion (Lifshitz case): comparison of definition of ignition delay time.

In order to disseminate the differences in the chlorine sub-mechanisms the case of a reactive H_2/Cl_2 mixture is considered. Lifshitz and Schechner[18] present experimental ignition delay times from a shock tube experiment at different conditions. Pelucchi et al.[12] presented several comparisons of the Lifshitz data with their kinetic model and for different reaction rate constants. However for the scope of this study, comparisons between all mechanism are only made at atmospheric pressure. The different definition of ignition delay time provided some differences across the range of temperatures. For the Pelucchi et al.[12] kinetic model definitions based on the maximum temperature, maximum concentration of HCl and of 50% maximum concentration of HCl are displayed in figure 4. As the closest match to the numerical results by Pelucchi et al.[12] is based on the 50% definition, this metric was used for reporting of H_2/Cl_2 ignition delay times.
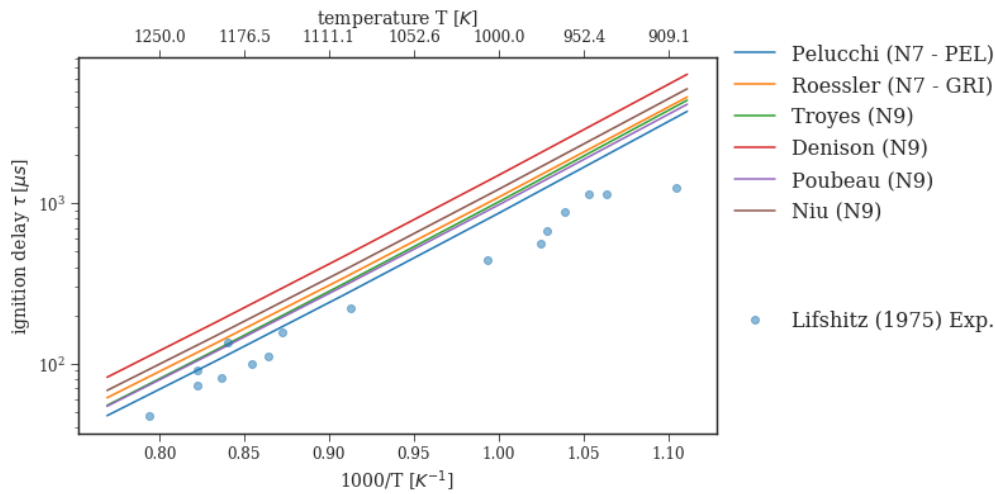
Figure 5: Ignition delay times for H_2/Cl_2 combustion (Lifshitz case).

The comparison of all the different kinetic models for this case is shown in figure 5. For all models, the estimated ignition delay times are approximately on the same order of magnitude and show a linear behaviour on the semilog scale. While the Pelucchi et al.[12] model is closest to the experimental data, experimental ignition delay time - especially at low temperatures - is generally lower by a factor of two. The Denison et al.[2] kinetic model shows the highest deviation and overpredicts ignition delay when compared to all other models. The relative simple chlorine sub-mechanism (6 reactions) used by Troyes et al.[5] performs almost as well as the Pelucchi et al.[12] model which contains 61 reactions in this subset. For this case the 7 reaction subset used by Poubeau et al.[6] performs similarly and only contains one more reaction pertinent to hydroperoxyl (HO_2) which is a species not considered by Troyes. When tested against the Pelucchi model for other mixture compositions the difference across the range of temperatures remained between 15% and 35% for both Troyes and Poubeau (see figure 6).

Figure 6: Relative difference in ignition delay times for H_2/Cl_2 between detailed and reduced mechanisms for selected cases.

2.4 Reactive H_2/air mixture

As the differences in the chlorine sub-mechanism ignition delay times were rather small between most the kinetic models considered, the subsets responsible for the hydrogen combustion pathways are examined by comparing ignition delay times for a stoichiometric hydrogen-air mixture at sea level conditions.

The ignition delay times of stoichiometric hydrogen-air mixture for all previous mechanism considered in this
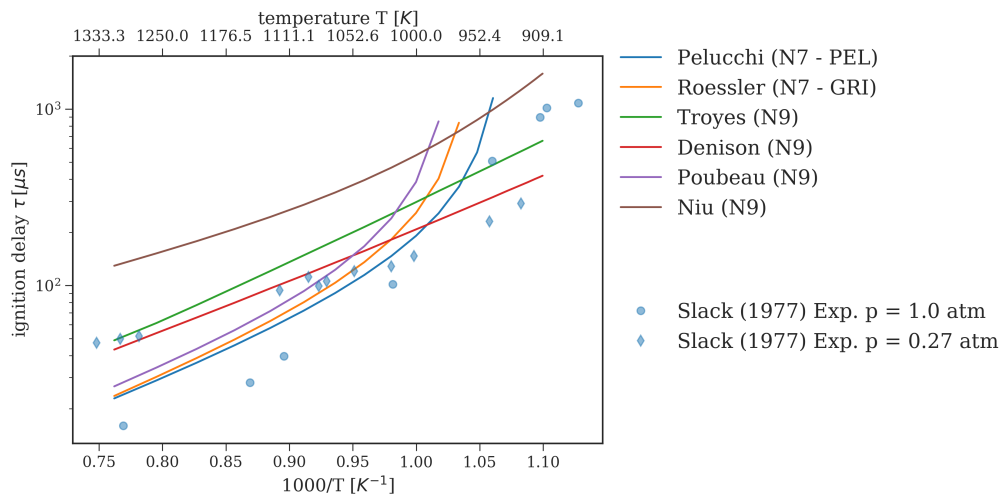
Figure 7: Ignition delay times for H_2/air combustion (Slack case).

study are shown in figure 7. It can be seen that both the hydrogen/oxygen submechanism employed by Troyes et al.,[5] Denison et al.[2] and Niu et al.[9] are unable to capture the transition from high-temperature kinetics to low-temperature kinetics at around 950 K. The more detailed mechanism are sophisticated enough to qualitatively show the transition, albeit all mechanism are not really close to the experimental data provided by Slack and Grillo.[19] As Zhukov[20] notes, the H_2, O_2 and HO_2 pathways are required for modeling a wide-temperature range. Possible mechanism which could provide improved hydrogen/oxygen pathways are the Jachimowski or abridged Jachimowski kinetic models.[20]

3. Improved skeletal kinetic model

Based upon the findings from the zero dimensional reactor studies an improved skeletal kinetic model based on the hydrogen/oxygen combustion pathways from the Jachimowski[21] with the carbonmonoxide/dioxide and chlorine pathways as implemented by Troyes et al.[5] is proposed. The complete skeletal mechanism which consists of 28 equations is displayed in table 3. Equations 1–19 represent the Jachimowski mechanism excluding the nitrogen reactions as proposed by Gerlinger.[22] The reduced carbon oxide (equations 20–22) and the hydrogen/chlorine pathways (equations 23–28) were taken from Troyes et al.[5] due to their favorable performance for ignition delay time in hydrogen/chlorine mixtures.

3.1 Reactor and ignition time

In order to evaluate the performance of the new skeletal kinetic model, the moist CO/HCl combustion (Roessler reactor) case previously presented is used. A comparison of the ignition times over a wide range of temperatures between the two detailed models and the current model is shown in figure 8. It can be seen that on the low temperature side, the kinetics are modeled very closely to that of the detailed model by Pelucchi et al..[12] On the the high temperature side, the behaviour is closer to that of the Troyes et al.[5] kinetic model - at any case the model stays within the bounds set by the two detailed kinetic models. As the low temperature side is more crucial to SRM plume post combustion this could indicate a welcoming performance for application in SRM plumes at lower computational cost.

From the previous validation study we know that despite different ignition delay times, the temperature and reactor molar concentration predicted by the Pelucchi and Roessler model are almost identical. Therefore a comparison of the currently presented improved skeletal kinetic model for reactor properties are made with the (detailed) Peluchi model and the (reduced) Troyes model. The results of this comparison are displayed in figure 9. When comparing the three levels of detailing it is clear that improving on the hydrogen/oxygen pathways has a very beneficial impact on the overall performance. While there are still some differences in species composition during the reaction time, the new kinetic model delivers improved species composition and temperature predictions much closer to the detailed model than to the reduced - at reduced computational cost. While this improved model contains 65% more reactions than the computationally cheapest model (Troyes), it already has 25% fewer reactions than the model by Poubau and 39% fewer reactions than the model by Denison.

COMBUSTION MODELING IN SOLID ROCKET MOTOR PLUMES

Table 3: Current improved skeletal kinetic model. Units in cm, mol, cal, s.

No.	Reaction			A	n	E_a	Reference
					Rate constants		
1	$H_2 + O_2$	$\rightleftharpoons$	$HO_2 + H$	1.0000e+14	0.00	5.6000e+04	[22]
2	$H + O_2$	$\rightleftharpoons$	$OH + O$	2.6000e+14	0.00	1.6800e+04	[22]
3	$O + H_2$	$\rightleftharpoons$	$OH + H$	1.8000e+10	1.00	8.9000e+03	[22]
4	$OH + H_2$	$\rightleftharpoons$	$H_2O + H$	2.2000e+13	0.00	5.1500e+03	[22]
5	$2\,HO$	$\rightleftharpoons$	$H_2O + O$	6.3000e+12	0.00	1.0900e+03	[22]
6^a	$H + OH + M$	$\rightleftharpoons$	$H_2O + M$	2.2000e+22	-2.00	0.0000e+00	[22]
7^b	$2\,H + M$	$\rightleftharpoons$	$H_2 + M$	6.4000e+17	-1.00	0.0000e+00	[22]
8^c	$H + O + M$	$\rightleftharpoons$	$OH + M$	6.0000e+16	-0.60	0.0000e+00	[22]
9^d	$H + O_2 + M$	$\rightleftharpoons$	$HO_2 + M$	2.1000e+15	0.00	-1.0000e+03	[22]
10	$HO_2 + H$	$\rightleftharpoons$	$2\,HO$	1.4000e+14	0.00	1.0800e+03	[22]
11	$HO_2 + H$	$\rightleftharpoons$	$H_2O + O$	1.0000e+13	0.00	1.0800e+03	[22]
12	$HO_2 + O$	$\rightleftharpoons$	$O_2 + OH$	1.5000e+13	0.00	9.5000e+02	[22]
13	$HO_2 + OH$	$\rightleftharpoons$	$H_2O + O_2$	8.0000e+12	0.00	0.0000e+00	[22]
14	$2\,HO_2$	$\rightleftharpoons$	$H_2O_2 + O_2$	2.0000e+12	0.00	0.0000e+00	[22]
15	$H + H_2O_2$	$\rightleftharpoons$	$H_2 + HO_2$	1.4000e+12	0.00	3.6000e+03	[22]
16	$O + H_2O_2$	$\rightleftharpoons$	$OH + HO_2$	1.4000e+13	0.00	6.4000e+03	[22]
17	$OH + H_2O_2$	$\rightleftharpoons$	$H_2O + HO_2$	6.1000e+12	0.00	1.4300e+03	[22]
18^e	$H_2O_2 + M$	$\rightleftharpoons$	$2\,HO + M$	1.2000e+17	0.00	4.5500e+04	[22]
19	$2\,O + M$	$\rightleftharpoons$	$O_2 + M$	6.0000e+13	0.00	-1.8000e+03	[22]
20	$CO + OH$	$\rightleftharpoons$	$CO_2 + H$	1.5000e+07	1.30	-7.6500e+02	[5]
21	$CO + O_2$	$\rightleftharpoons$	$CO_2 + O$	2.5300e+12	0.00	4.7700e+04	[5]
22^f	$CO + O + M$	$\rightleftharpoons$	$CO_2 + M$	2.5100e+13	0.00	-4.5400e+03	[5]
23	$HCl + H$	$\rightleftharpoons$	$H_2 + Cl$	2.3000e+13	0.00	3.5000e+03	[5]
24	$Cl_2 + H$	$\rightleftharpoons$	$HCl + Cl$	8.5900e+13	0.00	1.1700e+03	[5]
25	$HCl + OH$	$\rightleftharpoons$	$H_2O + Cl$	2.4500e+12	0.00	1.1000e+03	[5]
26	$HCl + O$	$\rightleftharpoons$	$OH + Cl$	5.2400e+12	0.00	6.4000e+03	[5]
27	$Cl + Cl + M$	$\rightleftharpoons$	$Cl_2 + M$	2.3400e+14	0.00	-1.8000e+03	[5]
28	$H + Cl + M$	$\rightleftharpoons$	$HCl + M$	7.2000e+21	-2.00	0.0000e+00	[5]

^{a}H_2O = 6.0
^{b}H_2 = 2.0, H_2O = 6.0
^{c}H_2O = 5.0
^{d}H_2 = 2.0, H_2O = 16.0
^{e}H_2O = 15.0
^{f}CO_2 = 3.8, CO = 1.9, H_2 = 2.5, H_2O = 12.0

3.2 Counter flowing diffusion flame

A counter flowing diffusion flame, also called laminar diffusion is generally referred to as a pure diffusion flame. Usually it describes a setup where two opposing stream of fuel and oxidant create a stagnation point at which combustion occurs (for setup and coordinate definition see figure 10). At the stagnation plane between the two streams where combustion occurs, the reaction rate is generally much higher than the molecular diffusion rate which is therefore rate governing.

Table 4: Case parameters

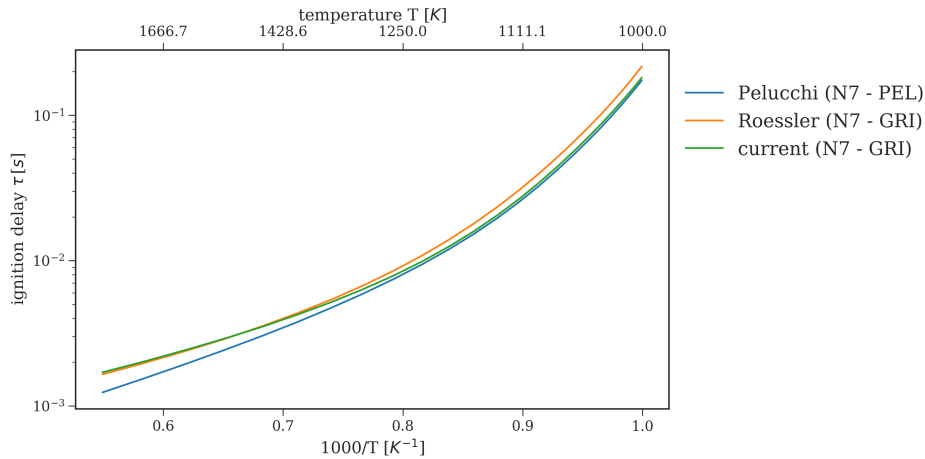| Variable	Value	species	mass fraction fuel	mass fraction oxidizer
pressure	0.9 atm	H_2O	0.2375	-
mass flux fuel	0.3 $kg/s/m^2$	HCl	0.2600	-
mass flux oxidizer	0.7 $kg/s/m^2$	CO_2	0.2579	-
gas temperature fuel	2400.0 K	CO_2	0.1427	-
gas temperature oxidizer	260.0 K	N_2	0.1020	0.7646
distance between inlets	0.02 m	O_2	-	0.2354

Figure 8: Ignition delay times for moist CO/HCl combustion (Roessler reactor case).
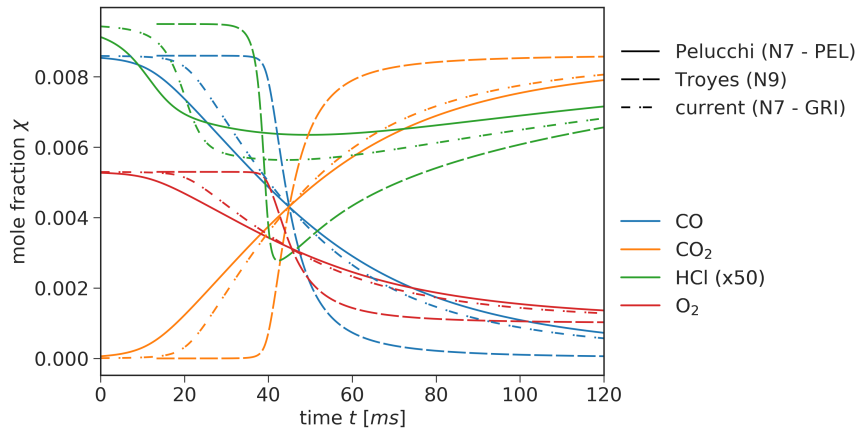
(a) Mole fractions of educts and products.
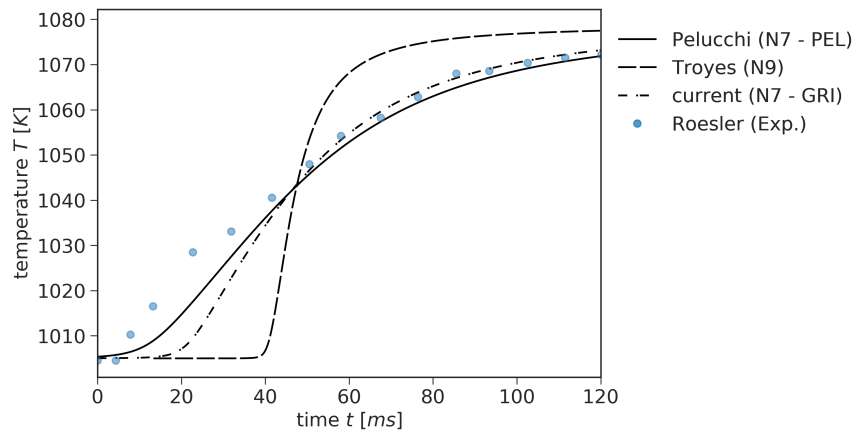
(b) Reactor temperature.

Figure 9: Reactor properties for moist CO/HCl combustion (Roessler reactor case) using the improved kinetic model.

For a (fuel) stream species composition representative of a SRM combustion chamber (H_2O/CO/HCl) opposing an stream (oxidizer) consisting of air, several studies using the different kinetic models were performed with the CANTERA toolbox. The boundary conditions for this counter flowing diffusion flame are shown in table 4.

The predicted species compositions on the stagnation plane are shown in figure 11. The figure bounds mark the fuel initial composition and the air initial conditions, on the left and respectively right side of the flame. Compared to

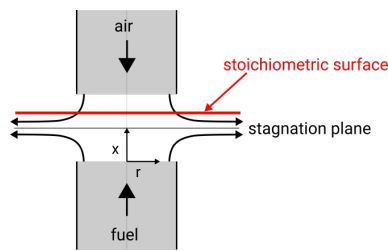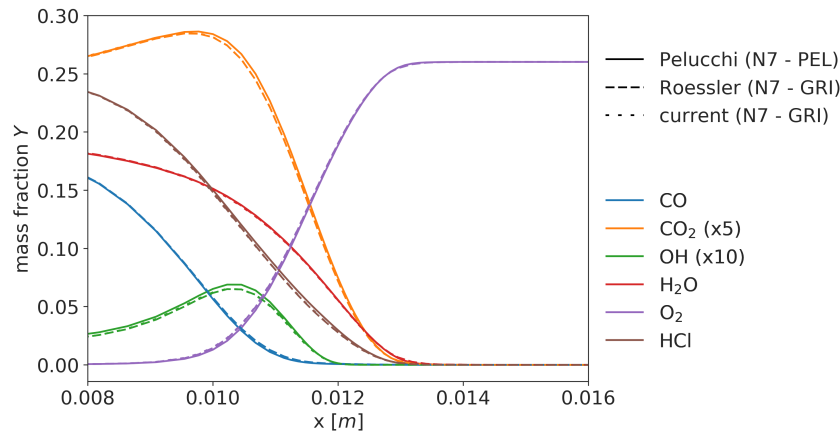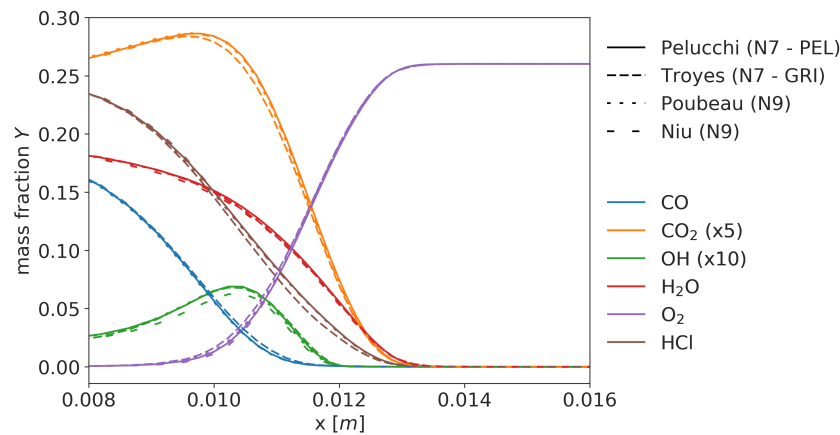COMBUSTION MODELING IN SOLID ROCKET MOTOR PLUMES

Figure 10: Counterflow diffusion flame geometry.

(a) Current model compared to detailed kinetic models.

(b) Roessler model compared to other reduced models.

Figure 11: Species composition profile in a counter flowing diffusion flame (H_2O/CO/HCl in air).

the reactor cases the differences between detailed Roessler et al. and reduced models are much less distinctive. As a mater of fact, only the Troyes kinetic model shows stronger deviations from the more detailed kinetics, most clearly visible in the hydrogen/carbon oxide species. However, when comparing the two detailed models - small differences between the Roessler et al. and the Pelucchi et al. model in the production of CO_2 within the flamefront arise.

Larger differences between the models are visible in the flame temperature profile which is displayed in figure 12. Between most detailed and most reduced kinetic model a temperature difference between peak values of approximately 80 K arises. The model by Poubeau, as well as the current skeletal model reach values slightly lower than the model by Roessler. The model by Pelucchi et al. shows the highest flamefront temperatures and a steeper falloff on the air side.
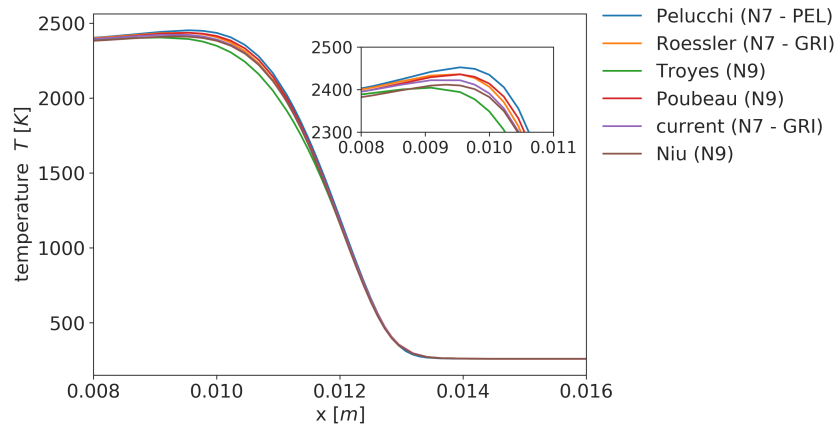
Figure 12: Temperature profile in a counter flowing diffusion flame (H_2O/CO/HCl in air).

4. Solid rocket motor plume

4.1 RANS applications

In a previous study[15] the influence of aluminum droplet evaporation, combustion and condensation on the inernal flow of a Bates type motor[23] was investigated. In the current study the focus lies on improving on the modeling of the SRM plume post combustion processes, therefore a motor without aluminum loading is considered. For this purpose several RANS calculations using different kinetic models are performed.
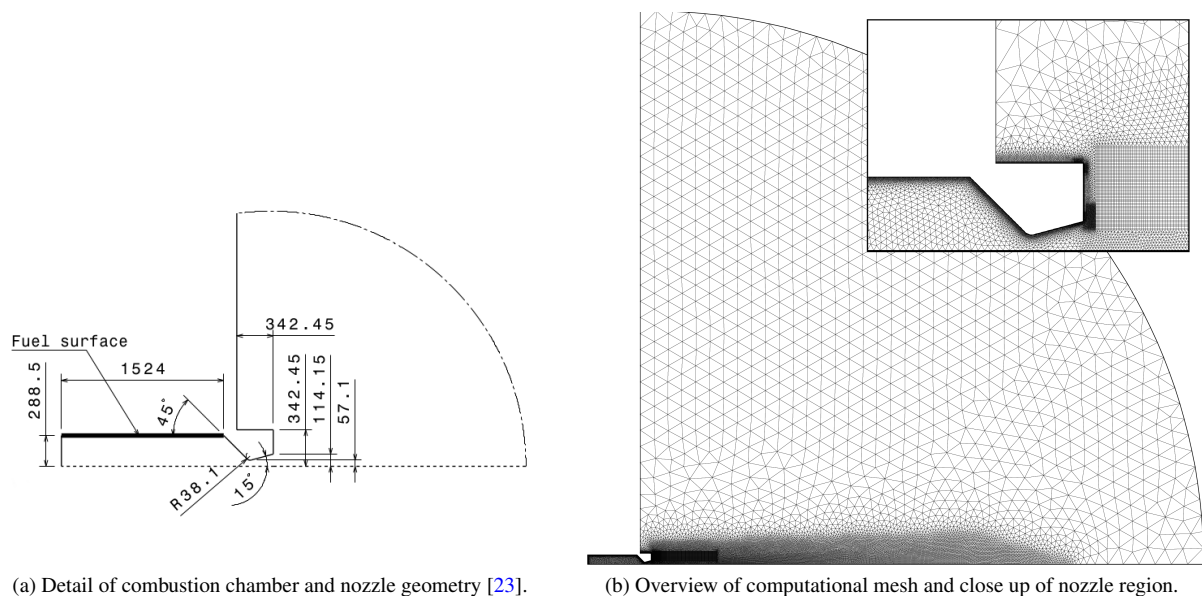
(a) Detail of combustion chamber and nozzle geometry [23].

(b) Overview of computational mesh and close up of nozzle region.

Figure 13: Numerical domain.

All numerical investigations in the framework of the present study were performed with the hybrid structured/unstructured DLR-Navier-Stokes solver TAU,[24] which is validated for a wide range of steady and unsteady sub-, trans- and hypersonic flow cases. The TAU code is a second order finite-volume solver for the Euler and Navier-Stokes equations in the integral form using eddy-viscosity, Reynolds-stress or detached- and large eddy simulation for turbulence modeling. The AUSMDV flux vector splitting scheme was applied together with MUSCL gradient reconstruction to achieve second order spatial accuracy. For turbulence modeling the k-ω SST model as introduced by Menter[25] is applied. The fuel walls were modelled with an effusion mass flux boundary condition which introduces the products of the solid combustion process at a pure radial velocity component. Currently the turbulence modelling is not modified to account for blowing effects at the wall.

COMBUSTION MODELING IN SOLID ROCKET MOTOR PLUMES

Table 5: Case parameters

Variable	Value	Variable	Value
chamber pressure	48.25 bar	co-flow Mach number	0.8
mass flux (fuel)	13.8295 $kg/s/m^2$	co-flow density	1.225 kg/m^3
gas temperature	2674.28 K	co-flow pressure	1.0 bar
nozzle wall temperature	1000.0 K	outside wall temperature	1000.0 K

Table 6: Input species mass fraction.

species	mass fraction	species	mass fraction
HCl	2.5555e-01	CO_2	1.4279e-01
CO	2.5307e-01	N_2	9.9524e-02
H_2O	2.3307e-01	H_2	1.0908e-02

The external and internal motor geometries are based on dimensions given by Sabnis et al..[23] The geometry was extended to include the external domain for the plume flow studies and is shown in figure 13. For the present case, the motor and freestream boundary conditions are given in table 5. The base flow conditions were estimated based on equilibrium conditions for the propellant formulation (AP/HTPB at 83.53%/16.47%) without aluminum contribution using the NASA CEA code (see table 6 for species distribution). The fuel wall temperature is set to 2674.28 K, which represents the flame temperature of the AP/HTPB mixture at 48 kPa chamber pressure. All other internal and external walls are set to 1000.0 K surface temperature. The external M = 0.8 co-flow is modeled as a freestream boundary condition with air properties at sea level conditions.

Several of the kinetic models previously presented are used to calculate finite rate chemistry for the SRM plume test case. The Troyes model is used as it is the computationally most affordable, representing the low side of complexity, the Roessler model is used instead of the Pelucchi model to obtain results using detailed chemistry. Both models are compared to results from the proposed improved skeletal model. For comparison a non-reactive multi-species calculation is also performed.

The flowfield temperature for all cases are shown in figure 14. The temperature contours show a flow structure representative for a classical under-expanded supersonic jet with nozzle exit pressures much higher than the environmental static pressure. The flow expands and turns outwards and is then compressed through an oblique shock wave at x/D of about 6. A series of expansion and shock waves follows until the jet potential core breaks down at around x/D > 40. The comparison with the non-reactive case shows the large role post-combustion or afterburning plays for SRM plumes. For this fictive non aluminized AP/HTPB temperature of up 2200 K in the shear layer and up to 2400 K in the core breakdown region are reached. While all models show a generally similar prediction of the plume temperature, some differences exist. The more detailed model by Roessler shows a distinctively higher shear layer temperature by about 75 – 100 K with peak spots located above the first shock and in the break down region. The proposed skeletal model gives a prediction of these hot flow features closer to the detailed model.

The temperature and species concentration on the centerline are displayed in figure 15. For both the species distribution and the temperature the general trends between the different models do not differ dramatically and are in line with previously reported CFD studies on SRM plumes.[2,5,8] However, as there is only very little oxygen in this core region large differences in this zone were not expected. At x/D > 30 when more and more oxygen mixes into the core region, combustion within this region is started. It is within this region where differences between the models are most obvious. Again, the proposed model predicts the kinetics very closely to the more detailed Roessler model.

The distribution of the Hydroxyl radical (OH) and HCl, both which are representative of partially intermittent products of the SRM chemistry, are shown for the reactive flow in figures 16 and 17 respectively. The OH concentration peaks in the growing shear layer starting from slightly above the nozzle lip line (r/D > 1.5) until jet potential core breakdown. The simpler Troyes model over predicts OH production both in the shear layer and especially close to the core breakdown region (x/D ~ 34–38) when compared to the more detailed Roessler model. The proposed kinetic model is very good in capturing most of the features present in the detailed model and also predicts lower OH concentration in the core breakdown region.

From the reactor studies it can be shown that the HCl mass fraction distribution is another indicator to evaluate these SRM plume kinetics. In difference to OH, which is only available in trace amounts within the SRM combustion chamber, HCl is one of the main products. Eventually, HCl is transferred trough several reactions to Cl and Cl_2 which can play a role in atmospheric ozone depletion.[2] A first peak of HCl is near the nozzle exit slightly above the lipline (r/D > 1.5). This peak is predicted by all three mechanism. However, the Roessler model shows a second region of high concentrations starting at x/D of 10, spanning up to x/D of 24. These regions are of relatively low temperature

(a) Inert species mixture.

(b) Troyes kinetic model.

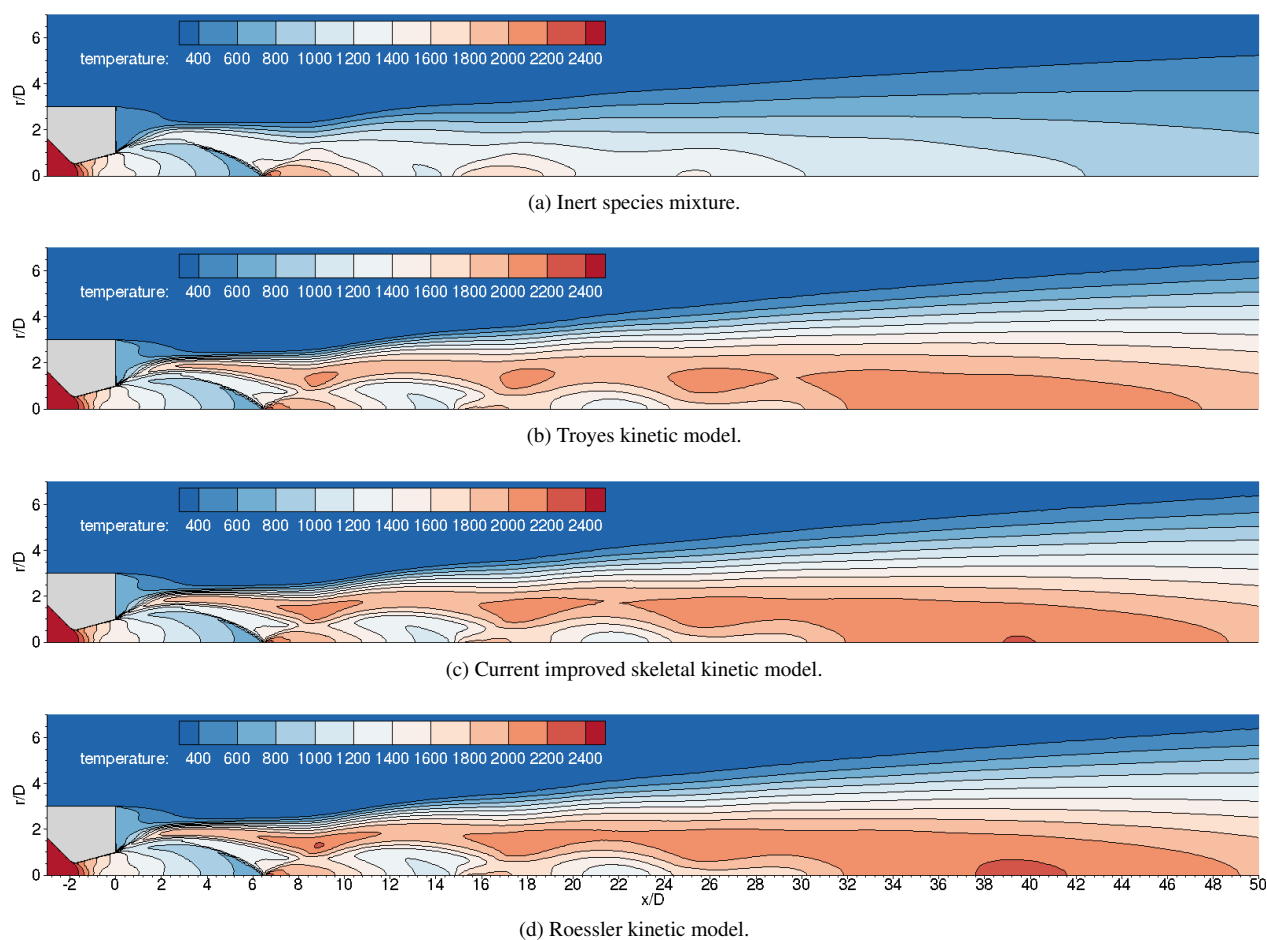(c) Current improved skeletal kinetic model.

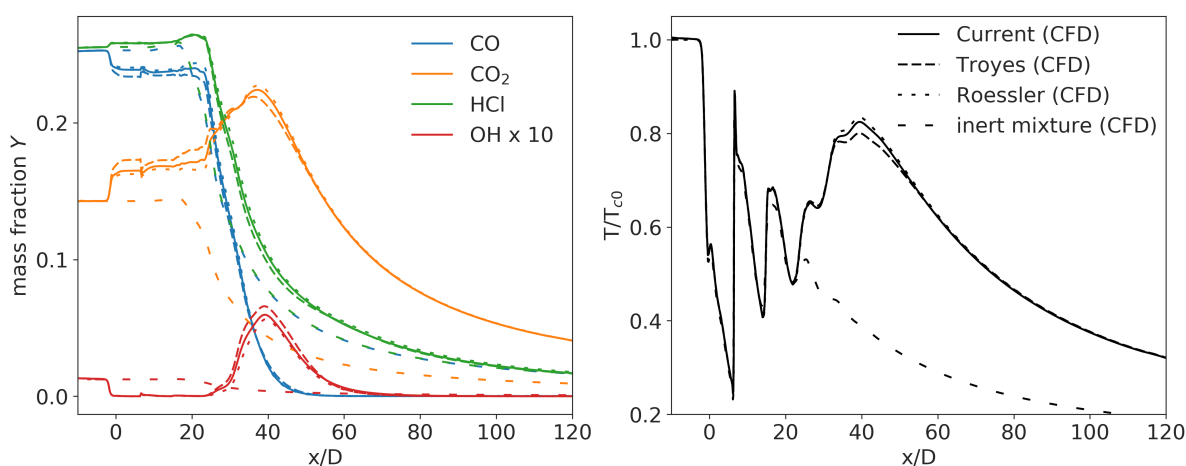(d) Roessler kinetic model.

Figure 14: Plume temperature.

Figure 15: Comparison of centerline properties.

located behind the expansion waves in the jet core (compare figure 14). As both the current proposed model and the Troyes model share the same chlorine mechanism, this indicates an important interaction between the chlorine reaction subset and the hydrogen/oxygen reaction subset. As was shown in the reactor studies, the Troyes kinetic model for hydrogen/combustion is too reduced to perform well in the low temperature regions.

Lastly the carbon-dioxide concentration within the plume is shown in figure 18. As CO_2 is one of the main species (along with CO and H_2O) with strong peaks in the spectrum (from $1000\,\mathrm{cm}^{-1}$ to $5000\,\mathrm{cm}^{-1}$),[8,26] the distribution in the plume is highly relevant. The Roessler model shows a peak of CO_2 concentration between at x/D of 34–40 with
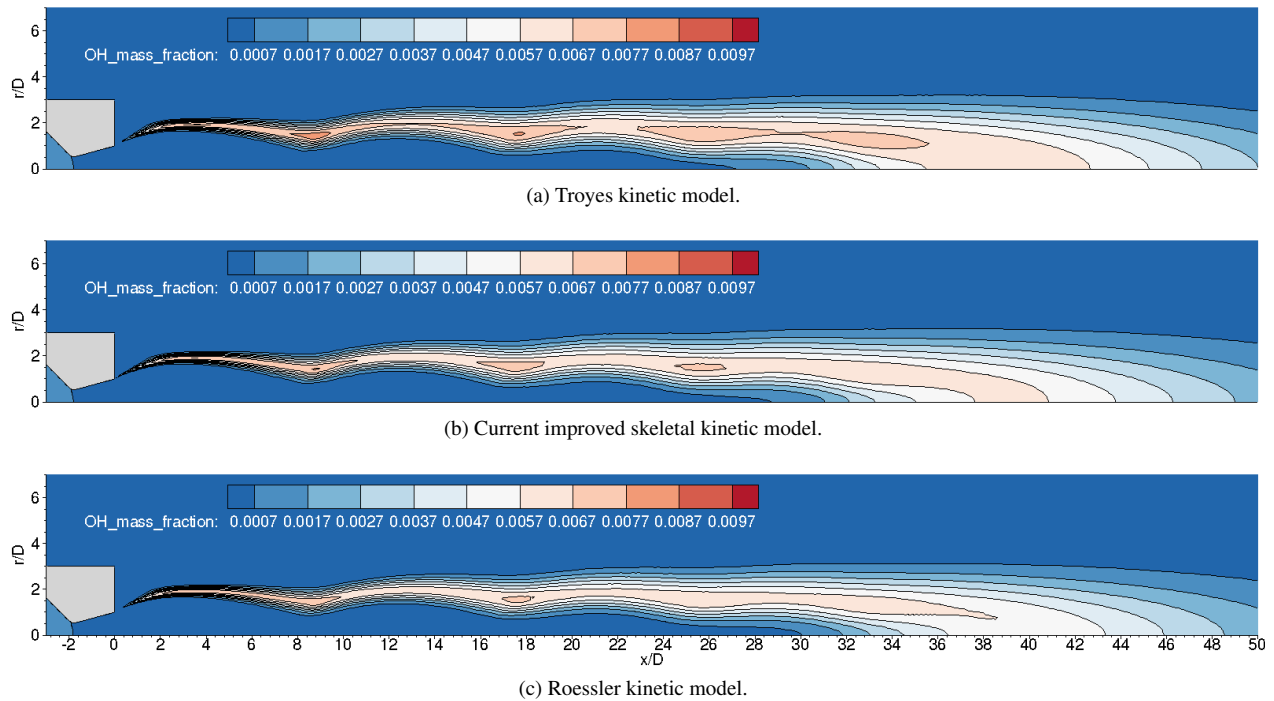
COMBUSTION MODELING IN SOLID ROCKET MOTOR PLUMES

(a) Troyes kinetic model.

(b) Current improved skeletal kinetic model.

(c) Roessler kinetic model.

Figure 16: Plume OH mass fractions.

(a) Troyes kinetic model.

(b) Current improved skeletal kinetic model.
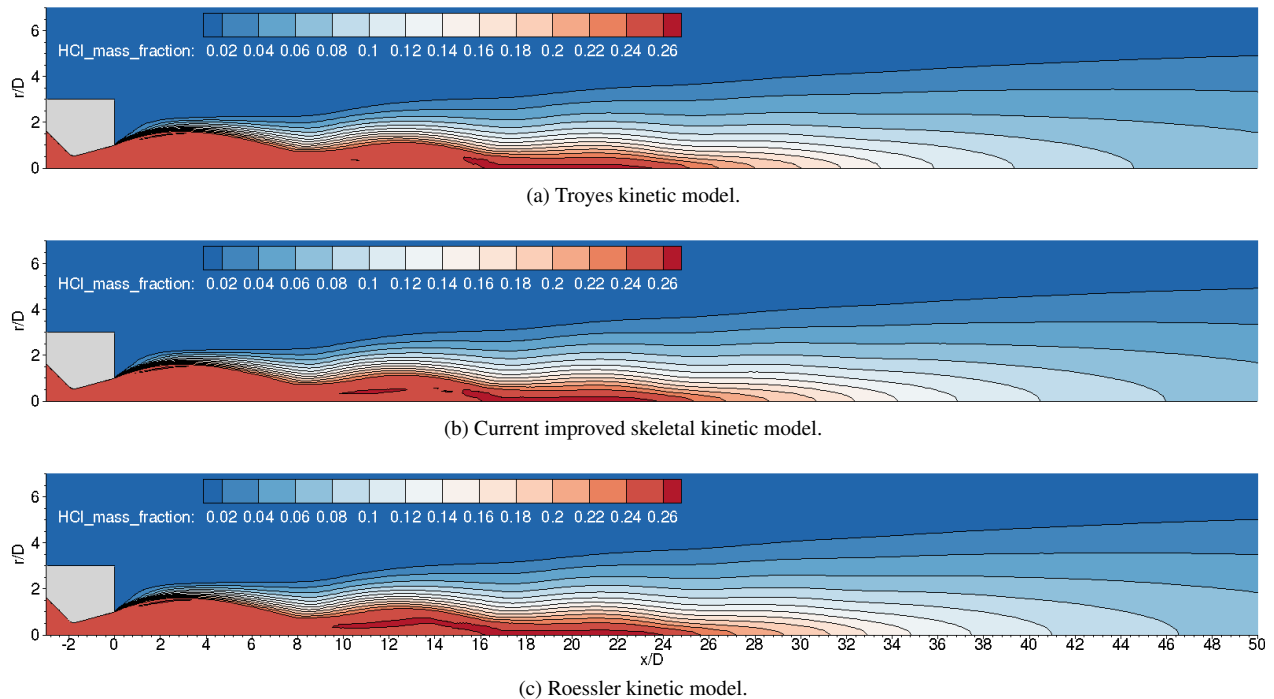

(c) Roessler kinetic model.

Figure 17: Plume OH mass fractions.

values up to 4% higher compared to the Troyes model. The difference between the models in temperature and CO_2 concentration on the centerline for this region is shown in figure 19. As CO_2 has a much higher IR absorption than CO this difference could influence the prediction of IR signatures of SRM plumes. Due to higher temperature, this effect on IR emissions would be enhanced. The proposed model reduces the difference in temperature and CO_2 prediction to around 1.5% of the absolute value.

(a) Troyes kinetic model.

(b) Current improved skeletal kinetic model.

(c) Roessler kinetic model.
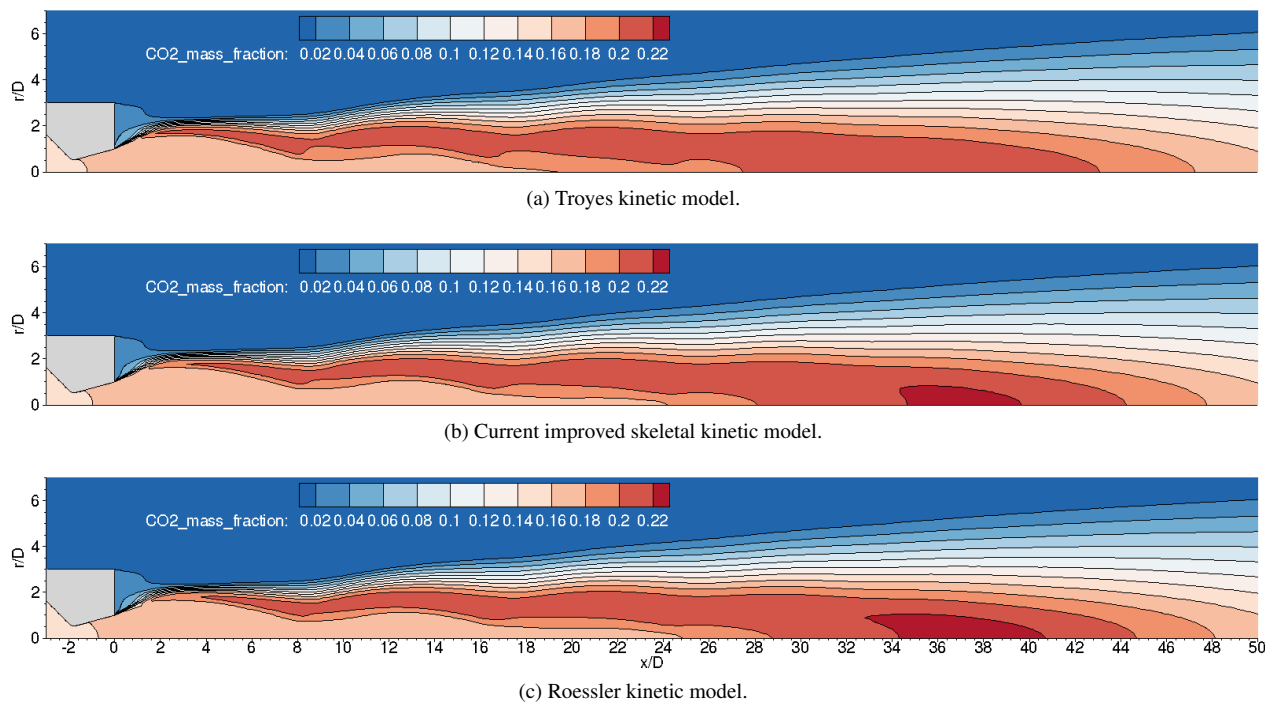
Figure 18: Plume CO2 mass fractions.
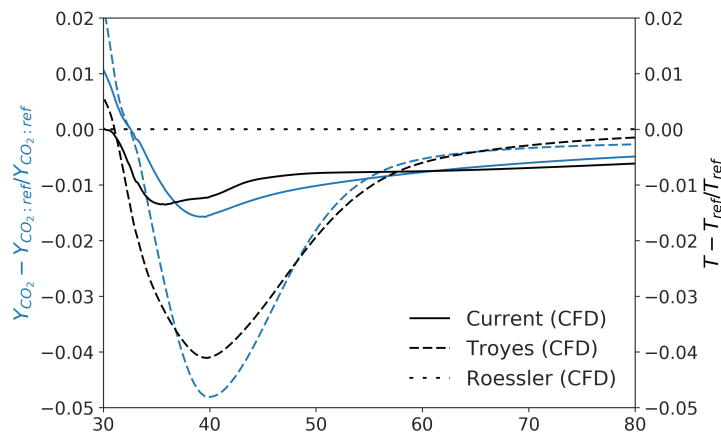
Figure 19: Comparison of model differences in CO_2 and temperature in core breakdown area.

5. Conclusions

The flow properties of solid rocket motor plumes are strongly influenced by complex hydrogen/oxygen/chlorine chemistry. Within this study we provided an overview on the available combustion mechanism and evaluate their applicability to SRM plumes using a constant volume reactor for moist CO/HCl, H_2/Cl_2 and a classic hydrogen/oxygen mixture. The results indicated that the choice of kinetic model subset for hydrogen/oxygen combustion may play a larger role in the oxygenated shear layers of the plume and may be less important in the hot potential core region.

Based on the evaluation an improved 28 reaction skeletal kinetic model is proposed and validated against detailed mechanisms. The applicability of the new kinetic model is tested with a SRM representative counterflowing diffusion flame and CFD calculations of a small scale Ammonium Perchlorate SRM plume test case. The presented results again highlight the large role afterburning plays for SRM plume thermochemistry. For the selected fictive non aluminized motor, temperatures of up 2200 K in the shear layer and up to 2400 K in the core breakdown region are reached. While all models show a generally similar prediction of the plume temperature and species distribution, some differences exist. The more detailed models show distinctively higher temperatures (75 – 100 K) in the shear layer and in the break down region.

Upstream of the core breakdown region, as more and more oxygen mixes into the core region, combustion within this region is started. It is within this region where differences between the models are most obvious. The OH concentration, which is an intermittent product in SRM combustion, peaks in the growing shear layer starting from slightly above the nozzle lip line until jet potential core breakdown. The simpler models over-predict OH production both in the shear layer and especially close to the core breakdown region when compared to the more detailed model. The proposed kinetic model is very good in capturing most of the features present in the detailed model and also predicts lower OH concentration in the core breakdown region. A first peak of HCl production appears near the nozzle exit at the binning of the shear layer. This peak is predicted by all investigated mechanism. However, the more detailed model shows a second region of high concentration starting behind the first expansion wave in the jet core, which are regions of relatively low temperature. Comparison between kinetic models indicates an important interaction between the chlorine reaction subset and the hydrogen/oxygen reaction subset. Lastly the carbon-dioxide shows peak concentration close to the core breakdown region, which is also where the highest plume temperatures are reached. The difference between the models in temperature and CO_2 concentration in this region are as much as 4.5 % which could impact IR emissions.

The proposed skeletal model gives a prediction of these hot flow features much closer to the detailed model at low computational costs and could be used for future scale-resolved simulations of multispecies, reactive solid-rocket motor plumes in order to predict plume thermochemistry, IR signature and environmental impact at launch sites.

References

[1]   M. N. Ross, J. O. Ballenthin, R. B. Gosselin, R. F. Meads, P. F. Zittel, J. R. Benbrook, and W. R. Sheldon. "In-situ measurement of Cl2 and O3 in a stratospheric solid rocket motor exhaust plume". In: *Geophysical Research Letters* 24.14 (July 1997), pp. 1755–1758. DOI: 10.1029/97GL01592.

[2]   M. R. Denison, John J. Lamb, William D. Bjorndahl, Eric Y. Wong, and Peter D. Lohn. "Solid rocket exhaust in the stratosphere - Plume diffusion and chemical reactions". In: *Journal of Spacecraft and Rockets* 31.3 (May 1994), pp. 435–442. DOI: 10.2514/3.26457.

[3]   Bernard Jeffrey Anderson and Vernon W Keller. *Space shuttle exhaust cloud properties*. NASA Technical Paper NAS 1.60:2258. NASA, 1983.

[4]   Thomas L. Jackson. "Modeling of Heterogeneous Propellant Combustion: A Survey". In: *AIAA Journal* 50.5 (May 2012), pp. 993–1006. DOI: 10.2514/1.J051585.

[5]   Julien Troyes, Isabelle Dubois, Vincent Borie, and Annie Boischot. "Multi-Phase Reactive Numerical Simulations of a Model Solid Rocket Exhaust Jet". In: *42nd AIAA/ASME/SAE/ASEE Joint Propulsion Conference & Exhibit*. American Institute of Aeronautics and Astronautics, July 2006. DOI: 10.2514/6.2006-4414.

[6]   Adèle Poubeau, Roberto Paoli, and Daniel Cariolle. "Evaluation of Afterburning Chemistry in Solid-Rocket Motor Jets Using an Off-Line Model". In: *Journal of Spacecraft and Rockets* 53.2 (Feb. 2016), pp. 380–388. DOI: 10.2514/1.A33311.

[7]   June Woo Lee, Jae Gwan Kim, and Kyu Hong Kim. "Effects of Al2O3 Particle on Convective and Radiative Heat Flux to Rocket Base Surface". In: *Seventh International Conference on Computational Fluid Dynamics (ICCFD7), Big Island, Hawaii*. July 2012.

[8]   V Rialland, A Guy, D Gueyffier, P Perez, A Roblin, and T Smithson. "Infrared signature modelling of a rocket jet plume - comparison with flight measurements". In: *Journal of Physics: Conference Series* 676.1 (2016), p. 012020.

[9]   Qinglin NIU, Zhihong HE, and Shikui DONG. "IR radiation characteristics of rocket exhaust plumes under varying motor operating conditions". In: *Chinese Journal of Aeronautics* 30.3 (2017), pp. 1101–1114. DOI: 10.1016/j.cja.2017.04.003.

[10] Jonathan M. Burt and Iain D. Boyd. "High Altitude Plume Simulations for a Solid Propellant Rocket". In: *AIAA Journal* 45.12 (2007), pp. 2872–2884. DOI: 10.2514/1.30129.

[11] J. F. Roesler, R. A. Yetter, and F. L Dryer. "Detailed Kinetic Modeling of Moist CO Oxidation Inhibited by Trace Quantities of HCl". In: *Combustion Science and Technology* 85.1-6 (Sept. 1992), pp. 1–22. DOI: 10.1080/00102209208947157.

[12] Matteo Pelucchi, Alessio Frassoldati, Tiziano Faravelli, Branko Ruscic, and Peter Glarborg. "High-temperature chemistry of HCl and Cl2". In: *Combustion and Flame* 162.6 (2015), pp. 2693–2704. DOI: 10.1016/j.combustflame.2015.04.002.

[13] GP Smith, DM Golden, M Frenklach, NW Moriarty, B Eiteneer, M Goldenberg, CT Bowman, RK Hanson, S Song, WC Gardiner, et al. *GRI-Mech version 3.0*. 1999.

[14] D.E. Jensen and G.A. Jones. "Reaction rate coefficients for flame calculations". In: *Combustion and Flame* 32 (1978), pp. 1–34. DOI: 10.1016/0010-2180(78)90078-0.

[15] Tobias Ecker, Sebastian Karl, and Klaus Hannemann. "Modeling of Aluminum Particle Combustion in Solid Rocket Combustion Chambers". In: *53rd AIAA/SAE/ASEE Joint Propulsion Conference, AIAA Propulsion and Energy Forum, (AIAA 2017-4781)*. July 2017. DOI: 10.2514/6.2017-4781.

[16] Volker Hannemann. *Numerical simulation of shock-shock-interactions considering chemical and thermal nonequilibrium*. DLR-Forschungsbericht 97-07, 1997.

[17] David G. Goodwin, Harry K. Moffat, and Raymond L. Speth. *Cantera: An Object-oriented Software Toolkit for Chemical Kinetics, Thermodynamics, and Transport Processes*. Version 2.3.0. 2017. DOI: 10.5281/zenodo.170284.

[18] Assa Lifshitz and Pinchas Schechner. "The mechanism of the H2 + CL2 reaction: Ignition behind reflected shocks". In: *International Journal of Chemical Kinetics* 7.1 (Jan. 1975), pp. 125–142. DOI: 10.1002/kin.550070113.

[19] M. Slack and A. Grillo. "Investigation of hydrogen-air ignition sensitized by nitric oxide and by nitrogen dioxide. Final report". In: *N-78-10233; NASA-CR-2896* (Oct. 1977).

[20] Victor P. Zhukov. "Validation, and Testing of Kinetic Mechanisms of Hydrogen Combustion in Fluid-Dynamic Computations". In: *ISRN Mechanical Engineering* 2012 (Feb. 2012). DOI: 10.5402/2012/475607.

[21] Casimir J. Jachimowski. *An analytical study of the hydrogen-air reaction mechanism with application to scramjet combustion [microform] / Casimir J. Jachimowski*. National Aeronautics, Space Administration, Scientific, and Technical Information Division, 1988.

[22] P Gerlinger, H. Moebius, and D. Brueggmann. "An Implicit Multigrid Method for Turbulent Combustion". In: *Journal of Computational Physics* 167.2 (2001), pp. 247–276. DOI: 10.1006/jcph.2000.6671.

[23] Jayant S. Sabnis. "Numerical Simulation of Distributed Combustion in Solid Rocket Motors with Metalized Propellant". In: *Journal of Propulsion and Power* 19.1 (2003), pp. 48–55. DOI: 10.2514/2.6101.

[24] S. Langer, A. Schwöppe, and N. Kroll. "The DLR Flow Solver TAU – Status and Recent Algorithmic Developments". In: *AIAA Paper AIAA-2014-0080*. 52nd Aerospace Sciences Meeting (2014). DOI: 10.2514/6.2014-0080.

[25] F. R Menter. "Two-Equation Eddy-Viscosity Turbulence Models for Engineering Applications". In: *AIAA Journal* 32.8 (1994), pp. 1598–1605. DOI: 10.2514/3.12149.

[26] Weichen Wang, Shipeng Li, Qiao Zhang, and Ningfei Wang. "Infrared radiation signature of exhaust plume from solid propellants with different energy characteristics". In: *Chinese Journal of Aeronautics* 26.3 (2013), pp. 594–600. DOI: 10.1016/j.cja.2013.04.019.